EUROPEAN ORGANIZATION FOR NUCLEAR RESEARCH

CERN-EP/83-20
3 February 1983

FORWARD-BACKWARD MULTIPLICITY CORRELATIONS IN $p\bar{p}$ COLLISIONS AT 540 GeV

UA5 Collaboration

(Bonn[1], Brussels[2], Cambridge[3], CERN[4], Stockholm[5])

K. Alpgård[5], R.E. Ansorge[3], B. Åsman[5], S. Berglund[5], K. Berkelman[4*], D. Bertrand[2], K. Böckmann[1], C.N. Booth[3], C. Buffam[4], L. Burow[1], P. Carlson[5], J.-L. Chevalley[4], B. Eckart[1], G. Ekspong[5], I. Evangelou[4**], J.-P. Fabre[4], K.A. French[3], J. Gaudaen[2***], C. Geich-Gimbel[1], M. Gijsen[4], K. von Holt[1], R. Hospes[1], D. Johnson[2], K. Jon-And[5], Th. Kokott[1], R. Mackenzie[4], M.N. Maggs[3], R. Meinke[1], Th. Müller[1], H. Mulkens[4], D.J. Munday[3], A. Odian[4†], J.G. Rushbrooke[3], H. Saarikko[1††], T. Saarikko[1], F. Triantis[4**], Ch. Walck[5], C.P. Ward[3], D.R. Ward[3], G. Weber[4†††], A.R. Weidberg[3], T.O. White[3], G. Wilquet[2] and N. Yamdagni[5]

1 Physikalisches Institut der Universität Bonn, Fed. Rep. Germany.
2 Inter-University Institute for High Energies (ULB-VUB), Brussels, Belgium.
3 Cavendish Laboratory, Department of Physics, Cambridge University, UK.
4 CERN, Geneva, Switzerland.
5 Institute of Physics, University of Stockholm, Sweden.

(Submitted to Physics Letters B)

---

*) Visiting scientist from Cornell University, Ithaca, NY, USA.
**) Visiting scientist from Ioannina University, Greece.
***) Also at the Universitaire Instellingen Antwerpen, Antwerp, Belgium.
†) Visiting scientist from SLAC, Stanford, Calif., USA.
††) Visiting scientist from Helsinki University, Finland.
†††) Visiting scientist from Hamburg University and DESY, Hamburg, Fed. Rep. Germany.

ABSTRACT

Results on correlations in charged multiplicity are presented using data from the UA5 detector at the CERN Super Proton Synchrotron collider. Both short-range and long-range correlations are observed. Our analysis gives no evidence for intrinsic long-range correlations. The observations are consistent with a physical picture in which small clusters are emitted at random along the rapidity axis in the plateau region. This result may indicate that random soft processes play a dominant role in high-energy hadronic collisions. The average cluster size is about two charged particles, the same as at Intersecting Storage Rings' energies. No variation of cluster size with multiplicity has been observed. The forward-backward long-range correlation and its energy dependence are related to the ratio of the first two moments, variance/mean, of the multiplicity distributions.

INTRODUCTION

A probe of the mechanisms of particle production in high energy reactions is the study of correlations among particles emitted at various values of rapidity, $y = 1/2 \ln [(E + p_L)/(E - p_L)]$. Many experiments have revealed a tendency for final state particles to be grouped in clusters over a range of rapidity of about one unit, which can be understood as the effect of resonance production [1].

Besides these short-range correlations, evidence exists from ISR experiments for correlations which extend over a longer range in rapidity and increase with energy [2]. The dynamical origin of these correlations is less clear. The CERN SPS collider offers an especially good opportunity for a study of such long-range correlations, since many particles are produced (on average 29 charged particles with an average density of about 3 charged particles per unit of pseudorapidity in the plateau region [3]), and since the rapidity range kinematically accessible (12 units) is much larger than that typical of short-range clustering effects. Based on a sample of about 4 000 minimum bias events we present here results on forward-backward charged particle multiplicity correlations in $\bar{p}p$ collisions at 540 GeV centre of mass energy.

APPARATUS

Charged particles were observed in the UA5 detector, which consists of two streamer chambers, placed symmetrically above and below the beam pipe. In the absence of momentum measurements (there was no magnetic field), we use pseudorapidity, $\eta = -\ln \tan \theta/2$, where θ is the angle of emission of a charged particle with respect to the beam axis. Although the two chambers cover the rapidity range $|\eta| < 5$ we have limited this investigation to a range where the overall geometrical acceptance was greater than 0.85, namely $|\eta| < 4$. The sample used has been corrected for the effects of secondary interactions, gamma conversions and decays. Single diffractive events are largely removed by the trigger. The triggering efficiency for non single diffractive inelastic events is estimated to be 95%. Further details on the apparatus and on the analysis can be found in our previous publications [3-7].

FORWARD-BACKWARD MULTIPLICITY CORRELATIONS

The influence of trivial correlations caused by kinematical constraints, such as phase space limits and energy-momentum conservation is avoided or at least diminished by using a restricted range of pseudorapidity, $|\eta| < 4$. Two symmetric, non-overlapping intervals in the pseudorapidity variable are defined, one forward (F) and one backward (B). For each event we determine the number of charged secondaries falling in the two intervals, n_F and n_B, and we define n_S as their sum.

Fig. 1a shows a scatter plot of events on the n_F, n_B plane for the case when F is $(0 < \eta < 4)$ and B is symmetric $(-4 < \eta < 0)$. As is seen from the accumulation of events near the diagonal $(n_F = n_B)$ the multiplicities in the two regions are correlated. The average value of the backward multiplicity at fixed forward multiplicity seems to be remarkably well described by a linear function of n_F (Fig. 1b), viz.

$$\langle n_B(n_F) \rangle = a + b n_F \, .$$

The slope b is a measure of the correlation strength between the multiplicities in the two intervals. The fitted value is $b = 0.54 \pm 0.01$. The value drops to $b = 0.41 \pm 0.01$ when a gap of width $\Delta\eta = 2$ is introduced between the two regions, so that F is $(1 < \eta < 4)$ and B is $(-4 < \eta < 1)$. The measured values are collected in Table 1, which also contains a value for b when F is restricted to the central part $(0 < \eta < 1)$ with B symmetric $(-1 < \eta < 0)$.

Table 1. Correlation strength b of the forward-backward multiplicity distribution for three different choices of rapidity intervals.

Rapidity interval	Correlation strength b
$\lvert\eta\rvert \leq 4$ (full range)	0.54 ± 0.01
$\lvert\eta\rvert \leq 1$ (central region)	0.48 ± 0.02
$1 \leq \lvert\eta\rvert \leq 4$ (full range with gap)	0.41 ± 0.01

The observed correlation strengths are significantly larger than at lower energies [2]. The energy dependence of b is shown in Fig. 2. The curves in the figure have been obtained from Monte Carlo simulations described further below.

The increase in value of the correlation parameter when the two regions are in contact can be mainly ascribed to the presence of short range correlations from clusters produced in the gap around $\eta = 0$ which often emit their charged decay products into both regions simultaneously. In support of this conjecture we observe two-particle correlations of short range as shown in Fig. 3. This shows the two-particle correlation function $\hat{C}_n(\eta_1, \eta_2)$ versus the rapidity difference between the two particles. The shape does not depend significantly on the multiplicity and is similar to that observed at lower energies [1, 2].

ANALYSIS OF LONG RANGE CORRELATIONS

We proceed to analyse the long range correlation which exists across the $\Delta\eta = 2$ gap. Such a gap should decouple the two regions from short range correlation effects. In the following F and B are defined symmetrically as $1 < |\eta| < 4$.

For our analysis we introduce in the scatterplot of events a new coordinate system rotated 45^o to the original axes. We first study the distribution of the combined multiplicity $n_S (= n_F + n_B)$ which has a mean $\langle n_S \rangle = 16.0 \pm 0.2$ and a dispersion $D_S = 8.8 \pm 0.1$. This corresponds to projecting all events onto the new n_S - axis in the scatter plot (not shown). From the way these moments, i.e. the mean $\langle n_S \rangle$ and the variance D_S^2, are defined, it is obvious that they contain no information as to how the particles in the events are distributed into the F and B regions. Formally there exists, for each n_S, a distribution $f_S(n_F)$ describing the probability of finding events with n_F particles in the F-region. As an example of $f_S(n_F)$ we have projected out of the scatter plot the sample of events for which $n_S = 12$ (185 events, Fig. 4). Obviously, $f_S(n_F)$ has to be symmetric around its mean and the position of the mean is at $n_F = \frac{1}{2} n_S$, properties imposed by our definitions of F and B and the symmetry of the initial state ($\bar{p}p$). Otherwise our selection imposes no further constraints

on the shape of the set of functions $f_S(n_F)$. It turns out that the correlation parameter b depends only on the second moments $d_S^2(n_F)$ of the f_S-distributions. One can show*) that the following identity holds between expectation values:

$$b = \frac{\frac{1}{4} D_S^2 - \langle d_S^2(n_F) \rangle}{\frac{1}{4} D_S^2 + \langle d_S^2(n_F) \rangle} ,$$

where the symbol $\langle x \rangle$ means an average of x over the n_S-distribution.

Various physical processes will control the shape of the $f_S(n_F)$ distributions in different ways. Some extreme processes might give rise to very narrow distributions and thus a large correlation parameter, other extreme processes might cause broad distributions resulting in small or even negative b-values. We first discuss two cases of intrinsic long range correlations. If two fireballs were emitted in opposite directions, decaying with highly correlated multiplicities, the resulting shape of the f_S-distribution would be very narrow and peaked at the symmetry point. If, on the other hand, many particles were produced on one of the sides (F or B) in correlation with few particles on the other side, the resulting f_S-distribution would be doubly peaked with a minimum at the symmetry point and b would be small or even negative. However, if the decay of the fireballs were uncorrelated as in double diffraction and non overlapping in rapidity, the b-parameter would be zero and the f_S-distributions fairly broad. We do not observe any of these cases, which means that none of the discussed processes dominates. However, we cannot exclude the possibility that a suitable mixture of such processes can give rise to the observed distributions and thus explain the observed b-parameter.

---

*) For a proof of the formula one notes that a least squares estimate of b with equal weight to all events gives $b = \mathrm{cov}(n_F, n_B)/\mathrm{var}\, n_F$. If the sums over all events implied by the variance and covariance are carried out in the two steps (i) over events with fixed n_S, (ii) over the n_S-distribution, the formula results.

We now consider additional physical pictures with no intrinsic long range correlation. An extreme case would be random emission of single particles along the rapidity axis. The shape of $f_S(n_F)$ is then binomial with probability $p = \frac{1}{2}$ for a track to fall in either region (F or B) and a dispersion given by $d_S^2(n_F) = p(1-p)n_S = \frac{1}{4}n_S$. In this case the correlation parameter is predicted by the identity formula to be 0.66, much higher than the observed value (0.41). This discrepancy arises because the binomial distribution (Fig. 4) is too narrow. The observed variances, $d_S^2(n_F)$ are larger by a factor close to 2 as is seen in Fig. 5a. The enhancement factor is remarkably constant, almost independent of n_S. We have also checked that it is independent of the gap size between the two regions as long as it is more than about one unit of pseudorapidity.

A better description of the data is obtained if clusters rather than single particles are assumed to be emitted at random and thus to have a binomial distribution with probability $p = \frac{1}{2}$ to fall in the F-region. If all decay products remain inside the region, which is closer to the truth the larger the region is, one would have $d_S^2(n_F) = k^2 \cdot \frac{1}{4}C = \frac{1}{4}k \cdot n_S$ under the assumption that all the clusters have the same size (k). Here C is the number of clusters in the two regions combined. From the observed values of d_S in Fig. 5 a cluster size of $k = 2$ seems sufficient. However, in a more realistic picture there would be a mixture of sizes $k = 1, 2, 3$ etc. with a mean $\langle k \rangle$ and a dispersion d_k. Furthermore, due to the limited acceptance of the regions, cluster products will leak from and into the observed regions. To a large extent these leakages will be compensated for in the averages but generally not in the same event, which means that the fluctuations are affected. The observed dispersions d_S will therefore be smaller than the ideal values. One can see this effect in Fig. 5 where three different size F-regions have been studied.

MONTE CARLO SIMULATIONS

It is of interest to generate clusters of a mixture of sizes and compare with data in Fig. 5 and also to study how this affects the b-value (Fig. 2) and its energy dependence. A minimum of assumptions has been made in order to make the simulation transparent. The charged particle multiplicity distribution [8] was unfolded to yield the cluster multiplicity distribution. The unfolding procedure was carried out for a variety of average k-values around $k = 2$. The values of k were

assumed to follow a Poisson distribution truncated by excluding values $k = 0$ and $k > 5$, although the results are not critically dependent on this assumption. For each event the clusters were distributed uniformly in pseudorapidity. Thus no intrinsic long range correlation is assumed. Starting from the position in pseudorapidity of each cluster its decay products are assigned new positions in the neighbourhood using a gaussian distribution with the observed two-particle short-range correlation width. Finally, the numbers of charged particles accepted in the F- and B-regions are recorded for each event. In this way the dispersions $d_S(n_F)$ at fixed n_S can be evaluated for a number of assumed average cluster sizes as shown in Fig. 5. Obviously, only an average cluster size around 2 fits the data. The effective size parameter, defined by the relation $\langle d_S^2(n_F)\rangle = k_{eff}\,\langle n_S\rangle/4$ can be shown to be given by $k_{eff} = \langle k\rangle + d_k^2/\langle k\rangle$ in in the limit where leakages are negligible. It is to be noted that when the regions are made smaller than $\Delta\eta = 3$ the decrease in the number of fully contained clusters reduces k_{eff} in the observed sample and in the Monte Carlo sample (with fixed $\langle k\rangle = 2$) in much the same way. Our aim is not to derive a precise value for the average cluster size, but from our analysis we find that $\langle k\rangle$ has to be smaller than about 2.5 and that a value close to 2 is likely.

Our interpretation is that ordinary low mass particles and resonances (π, η, ρ, ω, K^*...) or small clusters of them are copiously produced. The independence of k_{eff} on total multiplicity, Fig. 5, supports a picture in which high multiplicities are caused by a large number of small clusters produced rather than a few large ones. The very highest multiplicities $n_S > 30$ will be studied in more detail when sufficiently large samples are available.

The Monte Carlo results for the $n_F - n_B$ scatter plot yield correlation parameters which agree with data only for the case when the average cluster size is about 2 (Fig. 2). Repeating the Monte Carlo procedure at ISR energies also yields cluster sizes around 2 charged particles in agreement with published data [2]. The Monte Carlo simulation gives the energy dependence of the correlation parameter b as shown in Fig. 2.

DISCUSSION

The identity for b can now be cast in its final form

$$b = \frac{D_S^2/\langle n_S\rangle - k_{eff}}{D_S^2/\langle n_S\rangle + k_{eff}} .$$

From this and the result that k_{eff} is the same at all energies (apart from leakage effects) it follows that the dependence of the correlation parameter b on beam energy has its origin mainly in the increase of the ratio $D_S^2/\langle n_S\rangle$ with energy which is related to the shape of the total multiplicity distribution. We repeat that the two moments, $\langle n_S\rangle$ and D_S^2, are independent of the partitioning of the particles into the F- and B-regions.

Our analysis of the data seems to be consistent with a physical picture in which many random soft processes give rise to ordinary stable particles, small mass resonances and possibly small clusters. It is interesting to note that this picture implies a strong correlation between photon and charged particle multiplicities, which is in agreement with our published result [6]. The above picture should be considered as representing the dominating mechanism and does not exclude other components, such as double diffraction, hard scattering, jets etc.

CONCLUSIONS

We observe both short range and long range multiplicity correlations in the plateau region between -4 to +4 in pseudorapidity. The two particle short range correlation function has a gaussian standard deviation of about one unit of pseudorapidity, similar to what is observed at lower energies. It is natural to assume these to be caused by the decay of low mass resonances or clusters. The long range correlation strength is much larger than at lower energies and remains strong even across a gap of two units of pseudorapidity. The $\Delta\eta = 2$ gap is sufficiently large to decouple the two observed regions from correlations caused by the decay of resonances because most small mass resonances are unable to emit decay products into both of the observed regions simultaneously. There is no evidence in our data for intrinsic long range correlations. The

physical picture which emerges is one with many low multiplicity resonances emitted at random along the rapidity plateau. The origin of the large correlation strength lies in the large dispersion (D) of the multiplicity distribution, or more precisely in the large $D^2/\langle n \rangle$ ratio. The increase of the correlation parameter b with energy is due to the increase of the above mentioned ratio. A limit of about 2.5 has been found on the average cluster size, and a value close to 2 charged particles is likely. We find that the bulk of the charged particles are produced from clusters with the same average size independent of observed multiplicity. A superposition of independent soft processes may play the dominant role in the collisions of two fast hadrons. Our study is not sensitive to rare processes.

ACKNOWLEDGEMENTS

We are indebted to the many members of the CERN staff, particularly from the SPS and EF Divisions, who have contributed to the success of the SPS Collider and of our experiment. From the Brussels group, thanks are due from D.B. and G.W. for the financial support of the Fonds National de la Recherche Scientifique and the Institut Interuniversitaire des Sciences Nucléaires, and from J.G. and D.J. to the Interuniversitaire Institut voor Kern Wetenschappen for financial support. We also acknowledge with thanks the financial support of the Bonn group by the Bundesministerium für Wissenschaft und Forschung, of the Cambridge group by the UK Science and Engineering Research Council, and of the Stockholm group by the Swedish Natural Science Research Council. Finally, we acknowledge the contribution of the engineers, scanning and measuring staff of all our laboratories.

REFERENCES

[1] G. Giacomelli and M. Jacob, Physics Reports 55 (1979) 1;
J. Whitmore, Physics Reports 27 (1976) 187;
L. Foa, Physics Reports 22 (1975) 1.

[2] S. Uhlig et al, Nucl. Phys. B 132 (1978) 15.
J. Benecke and J. Kühn, Nucl. Phys. B 140 (1978) 179.

[3] K. Alpgård et al, Phys. Lett. 107 B (1981) 315.

[4] K. Alpgård et al, Phys. Lett. 107 B (1981) 310.

[5] K. Alpgård et al, Phys. Lett. 115 B (1982) 65.

[6] K. Alpgård et al, Phys. Lett. 115 B (1982) 71.

[7] UA5 Collaboration, Phys. Scr. 23 (1981) 642.

[8] K. Alpgård et al, "Particle Multiplicities in $\bar{p}p$ Interactions at $\sqrt{s}$ = 540 GeV", Phys. Letters (to appear).

FIGURE CAPTIONS

Fig. 1 (a) Scatter plot of multiplicities n_B and n_F for the pseudorapidity intervals $F = (0 < \eta < 4)$ and $B = (-4 < \eta < 0)$. For each value of n_B, n_F the area of the circle is proportional to the number of events. The straight line is the linear regression line also plotted in (b).

(b) The average value of n_B, taken at fixed n_F, as a function of n_F.

Fig. 2 Measured forward-backward correlation strength b as a function of the c.m. energy for three different rapidity intervals. Lower energy data from the R 701 experiment are from Ref. [2]. The curves represent the results of the Monte Carlo simulations of the model with random emission of clusters of an average size of two charged particles. The full range corresponds to $0 < |\eta| < 4$ and the gap in (c) is $|\eta| < 1$.

Fig. 3 The two particle correlation function $(n-1)\,\hat{C}_n(\eta_1, \eta_2)$ averaged over the interval $|\eta_1 + \eta_2| < 4$ shown as a function of the pseudorapidity difference $\eta_1 - \eta_2$. This particular sample has observed multiplicities in the range 20-30, but other ranges in multiplicity show very similar behaviour. For the definition of the correlation function, see e.g. Ref. [1]. The curve in a gaussian fit to the data.

Fig. 4 The forward-backward distribution for $n_S = 12$. Filled circles are our data points (185 events). Open circles represent the expected binomial distribution on the assumption that each track has a probability of 1/2 to fall in either region.

Fig. 5 The dispersion $d_S(n_F)$ plotted as $4d_S^2(n_F)/n_S$ as a function of $n_S (= n_F + n_B)$ for three different forward-backward regions, all with a gap $(-1 < \eta < 1)$ between them. The size $\Delta\eta$ of the regions are given in the figure. The curves are results of Monte Carlo calculations for different average cluster sizes $\langle k \rangle$.

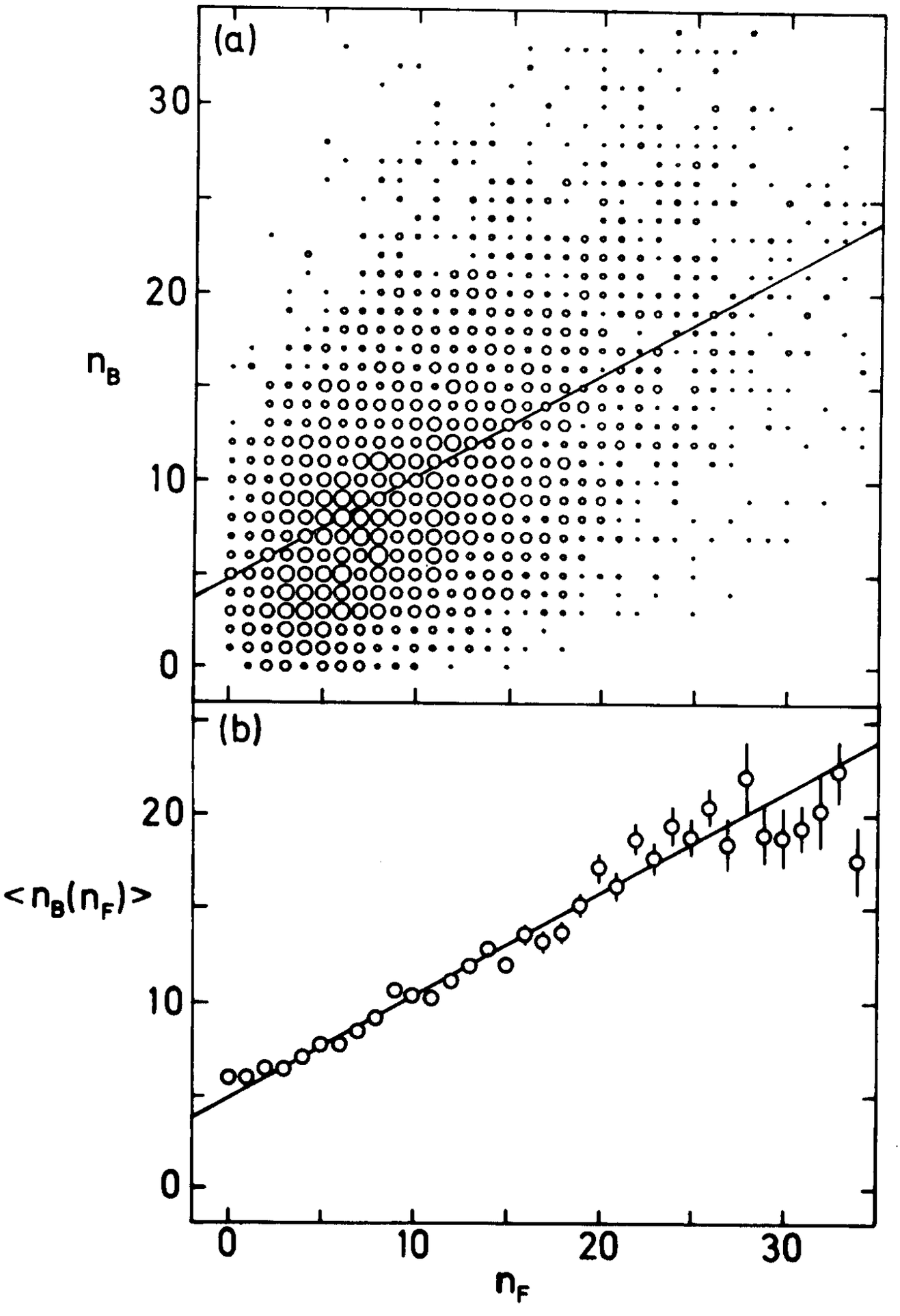

Fig. 1

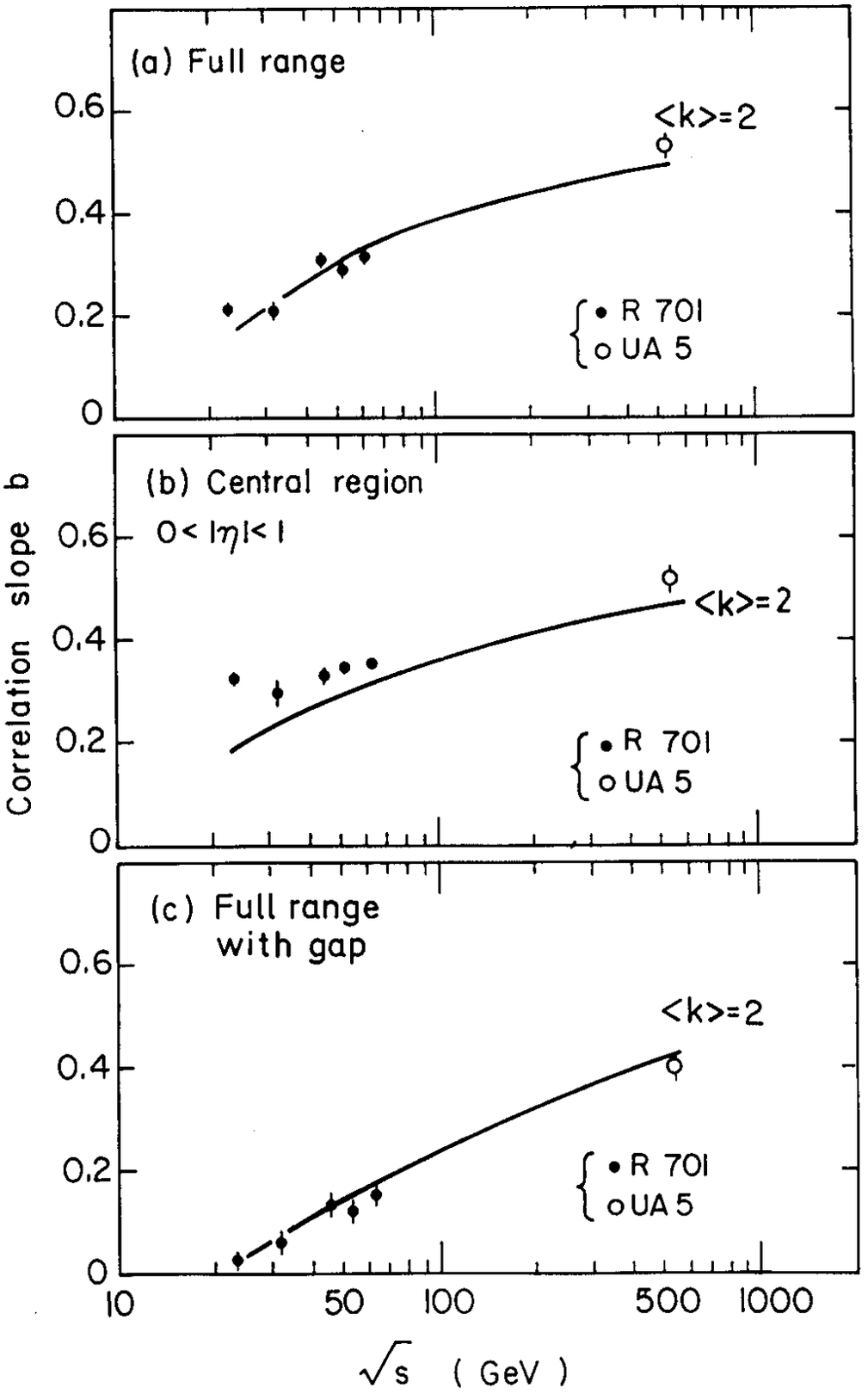
(a) Full range
<k>=2
• R 701
o UA 5
(b) Central region
0< |η|< 1
<k>=2
• R 701
o UA 5
(c) Full range
with gap
<k>=2
• R 701
o UA 5
Correlation slope b
0
0.2
0.4
0.6
10
50
100
500
1000
√s (GeV)

Fig. 2

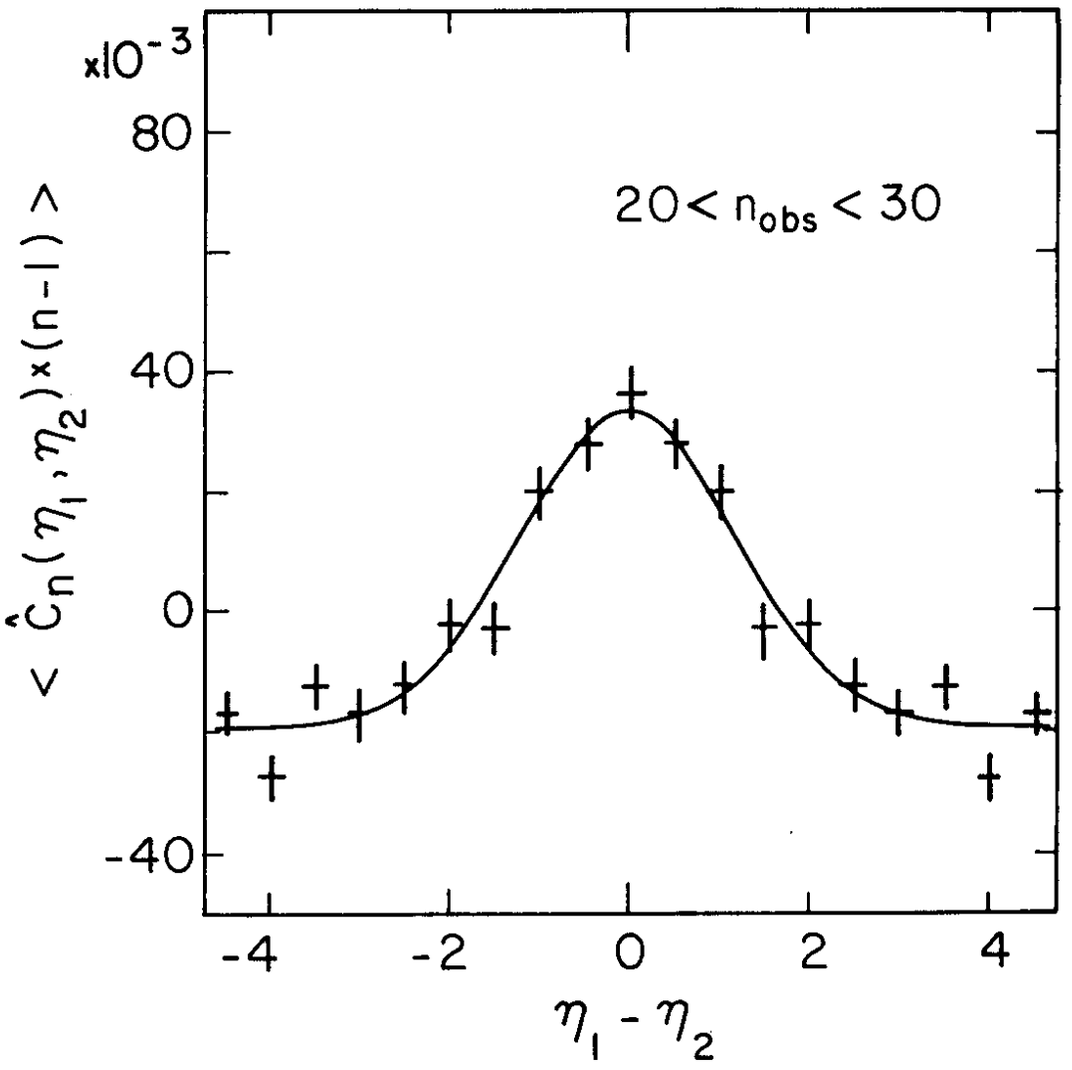

Fig. 3

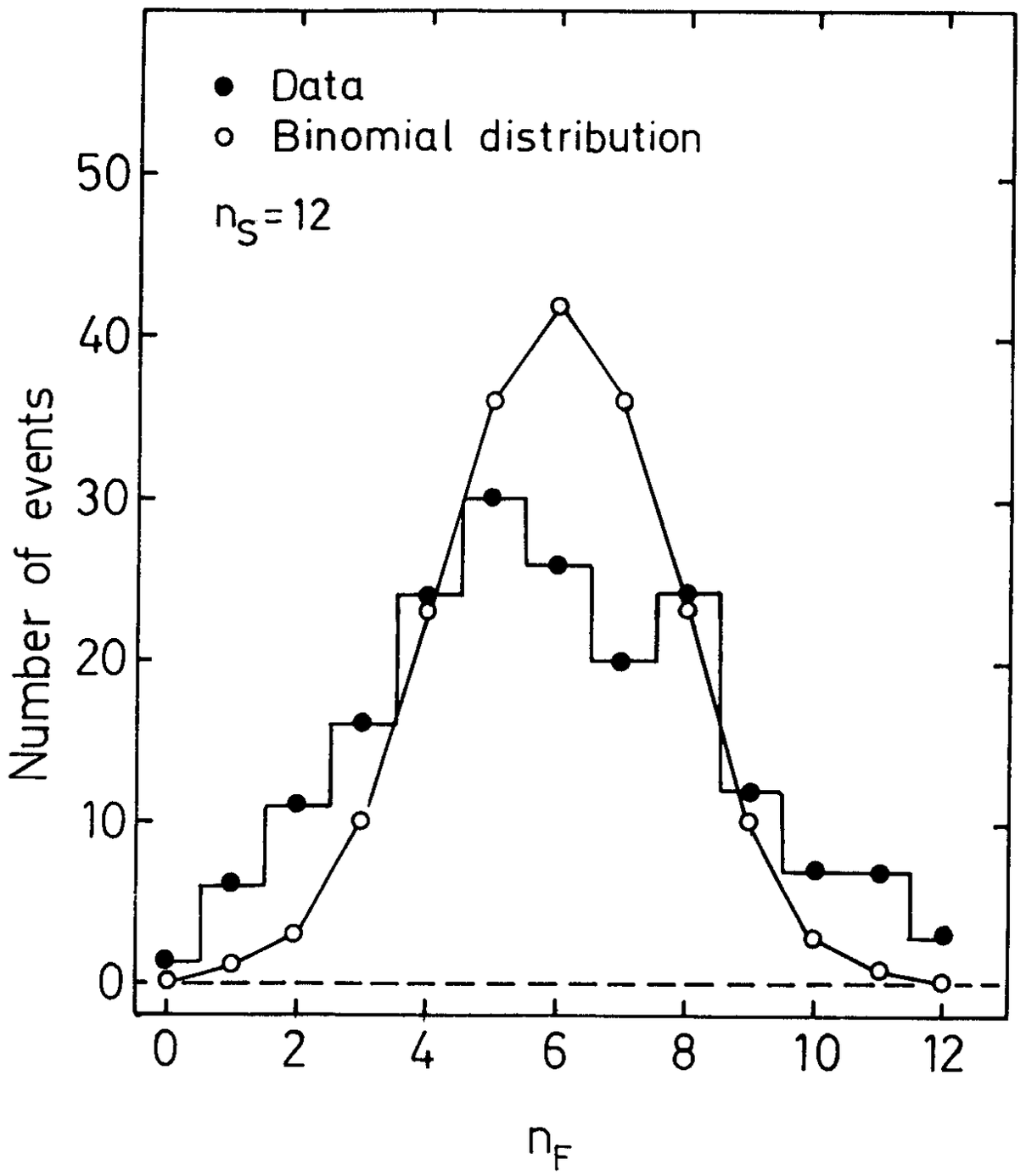
Data
Binomial distribution
$n_S = 12$
Number of events
50
40
30
20
10
0
0
2
4
6
8
10
12
n_F

Fig. 4

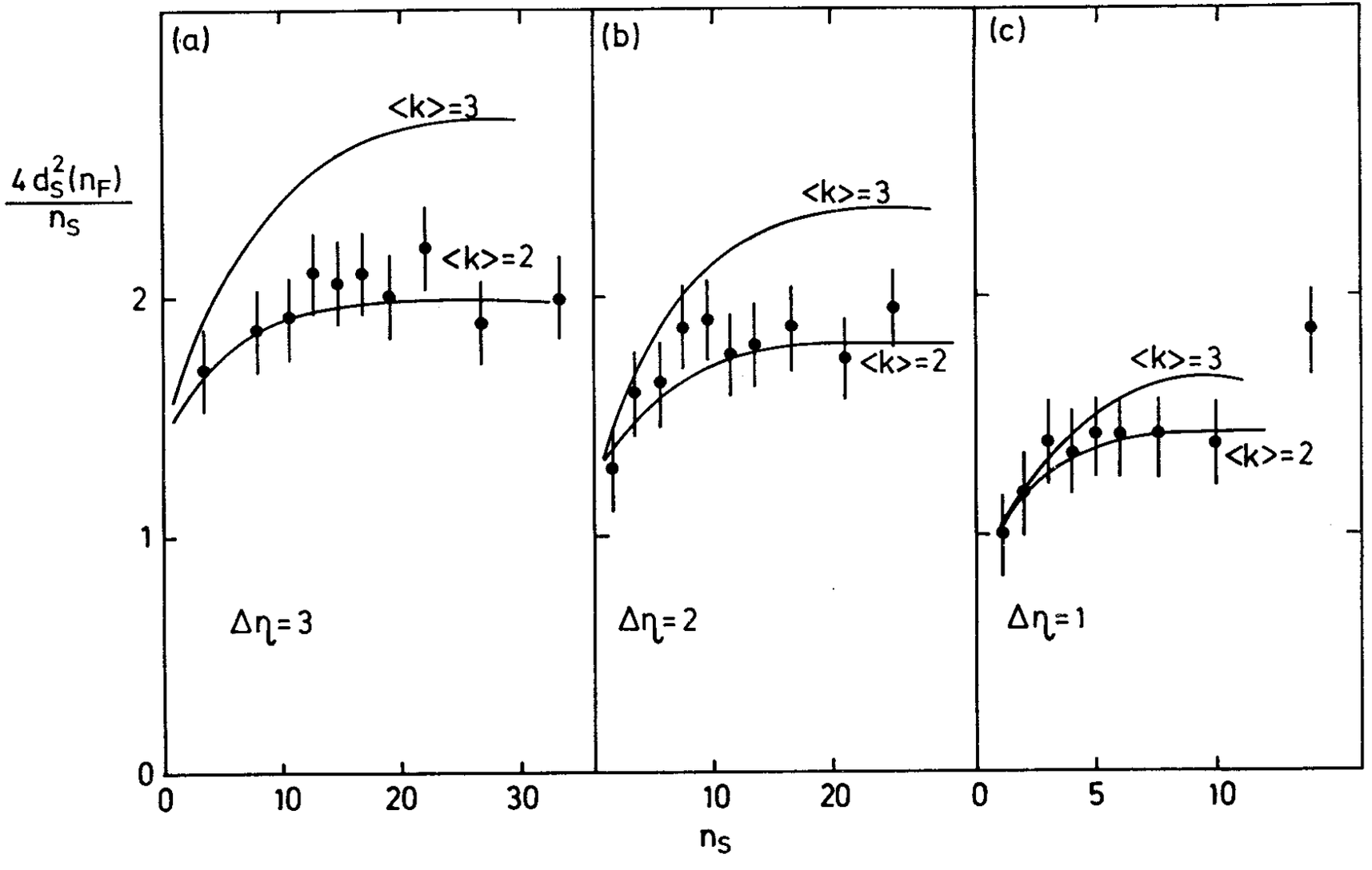
(a)
(b)
(c)
<k>=3
<k>=2
$\frac{4\,d_S^2(n_F)}{n_S}$
$\Delta\eta=3$
$\Delta\eta=2$
$\Delta\eta=1$
0
1
2
0
10
20
30
0
5
10
n_S

Fig. 5